Conformational Analysis of Poly(di-*n*-butylsilane), Poly(di-*n*-hexylsilane), and Poly(methyl-*n*-propylsilane) by a Rotational Isomeric State Scheme with Molecular Dynamics Simulations

Yuji Sasanuma,*,† Haruhisa Kato,† and Akira Kaito‡

Department of Materials Technology, Faculty of Engineering, Chiba University, 1-33 Yayoi-cho, Inage-ku, Chiba 263-8522, Japan, and Macromolecular Technology Research Center, National Institute of Advanced Industrial Science and Technology (AIST), AIST Tokyo Water Front, 2-41-6 Aomi, Kohtoh-ku, Tokyo 135-0064, Japan

Received: May 30, 2003; In Final Form: August 5, 2003

Conformational characteristics of poly(di-*n*-butylsilane) (PDBS), poly(di-*n*-hexylsilane) (PDHS), and poly(methyl-*n*-propylsilane) (PMPrS) have been investigated by a rotational isomeric state (RIS) scheme with molecular dynamics simulations. Characteristic ratios thus calculated for PDBS, PDHS, and atactic PMPrS are, respectively, 42.0, 54.0, and 12.3, being comparable to our light-scattering measurements. In the Θ state, most Si−Si bonds of PDBS and PDHS adopt deviant ± ($D_{\pm}$) conformations (dihedral angles ≈ ±150°); in adjacent Si−Si bonds, $D_{\pm}D_{\pm}$ conformations are the most stable, and $D_{\pm}D_{\mp}$ states have a slightly higher energy of ca. 0.1 kcal mol^{-1}. This is the reason for their rigidity in solution and the formation of a disordered structure. An RIS treatment for pseudoasymmetric polymers with different side chains (R and R′) (e.g., [-SiRR′-]$_x$ and [-CRR′-]$_x$) has been developed. By this method, the characteristic ratio of atactic PMPrS was obtained as above, and the stereosequence dependence of the spatial configuration of PMPrS was investigated; the characteristic ratio increases with the *meso*-diad probability. The UV absorption maxima (λ_{max}) of PDBS, PDHS, and PMPrS were correlated with average dihedral angles evaluated from the RIS calculations. The solubility of polysilanes has also been elucidated in terms of conformation.

1. Introduction

Polysilanes (PSs) are expected to be utilized for future optoelectronic devices because of their unique near-UV absorption and emission. The optical properties have been investigated in terms of thermochromism, solvatochromism, ionochromism, piezochromism, and so on.[1] The UV absorption and emission maxima have been found to vary with the main-chain conformation, which depends on the chemical species and length of the side chain.[1] Therefore, PSs should be good objects for molecular design; new materials may be developed according to the following scheme: desired physical properties ⟹ higher-order structures ⟹ primary structure ⟹ synthetic method. To establish this route, the structure−property relationships and correlations between primary and higher-order structures must be elucidated.

In our previous study,[2] the Θ conditions of poly(di-*n*-butylsilane) (PDBS), poly(di-*n*-hexylsilane) (PDHS), and poly(methyl-*n*-propylsilane) (PMPrS) were found, and the corresponding characteristic ratios $\langle r^2\rangle_0/nl^2$ were determined: PDBS, 42.3 in *n*-hexane at 19.1 °C; PDHS, 42.5 in a mixed solvent of *n*-hexane (58.2%) and 2-propanol (41.8%) at 25 °C; and PMPrS, 19.9 in *n*-hexane (62.6%) and 2-propanol (37.4%) at 25 °C. Here, r is the end-to-end distance, n is the number of skeletal bonds, l is the bond length, the angular brackets represent the ensemble average, and the 0 subscript stands for the unperturbed state. Figure 1 shows UV spectra observed from the Θ solutions and solid films of the three PSs.[2] Unperturbed PDBS, PDHS, and PMPrS show absorption maxima (λ_{max}values) at 314, 314, and 306 nm, respectively. The similarities in $\langle r^2\rangle_0/nl^2$ and λ_{max} between PDBS and PDHS suggest that both PSs adopt almost the same backbone conformations in the Θ state. Fresh solid films of PDBS and PDHS have the same λ_{max} values as the Θ solutions; however, the mature PDHS film exhibits another absorption (at 363 nm), which comes from the all-anti conformation (AAAAA...) induced by side-chain crystallization.[3−5] In the crystalline state, the PDBS chain takes the all-deviant $D_+D_+D_+D_+D_+$... (or $D_-D_-D_-D_-D_-$...) conformation with the same sign and hence forms a 7/3 helical structure.[6] It was also found that PDBS and PDHS in solution shift the UV absorption to 355 nm at −36 and −31 °C, respectively.[6,7] For PMPrS, the λ_{max} value changes from 306 to 329 nm by solidification.[2] In this paper, the nomenclature proposed by PS researchers[8] has been employed: anti (A), dihedral angle $\phi \approx 180°$; transoid (T), $\phi \approx 165°$; deviant (D), $\phi \approx 150°$; ortho (O), $\phi \approx 90°$; and gauche (G), $\phi \approx 60°$, where ϕ is defined according to the IUPAC recommendation.[9]

In this study, we have carried out conformational analyses of PDBS, PDHS, and PMPrS by the rotational isomeric state (RIS) scheme[10,11] to relate their chain configurations and conformations to higher-order structures and properties. The experimental $\langle r^2\rangle_0/nl^2$ data[2] were used as criteria to confirm the reliability of the analysis. The RIS scheme is a theoretical

* To whom correspondence should be addressed. E-mail: sasanuma@faculty.chiba-u.jp. Fax: +81 43 290 3394.
† Chiba University.
‡ AIST.

10.1021/jp030681v CCC: $25.00
Published on Web 10/08/2003

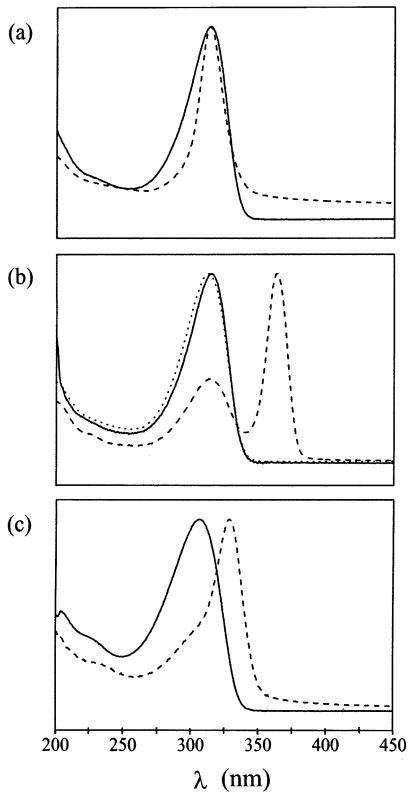

Figure 1. Ultraviolet absorption spectra of (a) PDBS, (b) PDHS, and (c) PMPrS: (—) θ solution, (•••) fresh film, (- - -) film after standing at room temperature for a day. (Adapted from ref 2.)

treatment that is successful in relating the chain conformation to configuration-dependent properties. However, the methodology has been restricted to molecular chains with short substituents because interactions between long flexible side chains and between main and side chains can scarcely be treated explicitly in the RIS scheme. Here, we have attempted to combine the RIS scheme with molecular dynamics (MD) simulations to enable conformational analyses of PSs with long side chains. In this paper, the methodology is described, and the results of the analysis are discussed in terms of side-chain species, stereosequences, solid-state structures, and thermal, optical, and solution properties.

2. Computational Procedure

2.1. Rotational Isomeric State Treatment for PS Chains. The RIS treatment for polymethylene[10,12] may be applied to poly(dimethylsilane) (PDMS), provided that the methyl substituent is considered to be a unit. To evaluate conformational energies and geometrical parameters of polymers, their oligomeric model compounds have often been employed. In the case of PDMS, the smallest model compound that gives both first-order (between atoms and groups separated by three bonds) and second-order (by four bonds) interactions is linear $Si_5(CH_3)_{12}$ (referred hereafter to as Si_5Me_{12}). In contrast to *n*-alkanes, which show a three-fold potential, Si_4Me_{10} and Si_5Me_{12} have six potential minima at $\phi \approx \pm 165°$ ($T_\pm$), $\pm 90°$ ($O_\pm$), and $\pm 55°$ ($G_\pm$).[13−15] Accordingly, the statistical weight matrices must be extended to 6×6. The applicability of the six-state model to PDBS, PDHS, and PMPrS will be shown later.

Statistical weight matrices (U_2 and U_i) for the second and ith ($i \geq 3$) Si−Si bonds may be given by[10,11]

$$U_2 = \begin{array}{c} \\ T_+ \\ T_- \\ O_+ \\ O_- \\ G_+ \\ G_- \end{array} \begin{array}{c} \begin{array}{cccccc} T_+ & T_- & O_+ & O_- & G_+ & G_- \end{array} \\ \begin{pmatrix} \sigma_{T_+} & \sigma_{T_-} & \sigma_{O_+} & \sigma_{O_-} & \sigma_{G_+} & \sigma_{G_-} \\ 0 & 0 & 0 & 0 & 0 & 0 \\ 0 & 0 & 0 & 0 & 0 & 0 \\ 0 & 0 & 0 & 0 & 0 & 0 \\ 0 & 0 & 0 & 0 & 0 & 0 \\ 0 & 0 & 0 & 0 & 0 & 0 \end{pmatrix} \end{array} \quad (1)$$

and

$$U_i = \begin{array}{c} \\ T_+ \\ T_- \\ O_+ \\ O_- \\ G_+ \\ G_- \end{array} \begin{array}{c} \begin{array}{cccccc} T_+ & T_- & O_+ & O_- & G_+ & G_- \end{array} \\ \begin{pmatrix} \sigma_{T_+T_+} & \sigma_{T_+T_-} & \sigma_{T_+O_+} & \sigma_{T_+O_-} & \sigma_{T_+G_+} & \sigma_{T_+G_-} \\ \sigma_{T_-T_+} & \sigma_{T_-T_-} & \sigma_{T_-O_+} & \sigma_{T_-O_-} & \sigma_{T_-G_+} & \sigma_{T_-G_-} \\ \sigma_{O_+T_+} & \sigma_{O_+T_-} & \sigma_{O_+O_+} & \sigma_{O_+O_-} & \sigma_{O_+G_+} & \sigma_{O_+G_-} \\ \sigma_{O_-T_+} & \sigma_{O_-T_-} & \sigma_{O_-O_+} & \sigma_{O_-O_-} & \sigma_{O_-G_+} & \sigma_{O_-G_-} \\ \sigma_{G_+T_+} & \sigma_{G_+T_-} & \sigma_{G_+O_+} & \sigma_{G_+O_-} & \sigma_{G_+G_+} & \sigma_{G_+G_-} \\ \sigma_{G_-T_+} & \sigma_{G_-T_-} & \sigma_{G_-O_+} & \sigma_{G_-O_-} & \sigma_{G_-G_+} & \sigma_{G_-G_-} \end{pmatrix} \end{array} \quad (2)$$

where σ_η represents the statistical weight for the first-order interaction energy E_η of the η state ($\eta = T_+, T_-$ ..., or G_-), and $\sigma_{\eta\eta'}$ is that for the first-order plus second-order interaction energy of the $\eta\eta'$ state ($\eta\eta' = T_+T_+, T_+T_-$..., or G_-G_-). The rows and columns of the matrices are indexed to rotational states for the preceding and current bonds, respectively. The two-dimensional energy $E_{\eta\eta'}$ of the $\eta\eta'$ state, evaluated from MD simulations as described later, includes two first-order interaction energies (E_η and $E_{\eta'}$) and one second-order interaction energy. The statistical weights σ_η and $\sigma_{\eta\eta'}$ are, respectively, calculated from $\sigma_\eta = \exp(-E_\eta/RT)$ and $\sigma_{\eta\eta'} = \exp[-(E_{\eta\eta'} - E_\eta)/RT]$, where R is the gas constant, and T is the absolute temperature.

As will be shown later, for PDBS and PDHS, the trans minima are located at ca. $\pm 150°$ ($D_\pm$), whereas trans positions of PMPrS, depending on the stereosequence, were found over a comparatively wide range (Supporting Information). In this paper, trans conformations (A, T, and D) are often represented only by T, as in eqs 1 and 2. If the energy and geometrical parameters are given, then the RIS scheme enables us to calculate various configuration-dependent properties of PS chains.

2.2. Pseudoasymmetry of PMPrS. Because PMPrS has asymmetric side chains of methyl and *n*-propyl groups, the first-order and second-order interaction energies are assumed to depend on up to tetrad and pentad configurations, respectively. According to the concept of pseudoasymmetry, which has been used for vinyl polymers,[10,11,16,17] 16 (2^4) tetrads and 32 (2^5) pentads can be enumerated for PSs such as $[-SiRR'-]_x$ (R and R′: side chains). Of the 32 pentads (Table 1), only 10 (*dldld*, *dldll*, *dlddl*, *dlddd*, *dllld*, *dllll*, *ddldd*, *ddlll*, and *ddddd*) are independent of each other. For definitions of the *d* and *l* forms[16,17] and the *meso* (*m*) and *racemo* (*r*) linkages,[18] see Figure 2. In the *d* and *l* representation of Table 1, the right-hand pentad (A′) corresponds to the mirror image of the left-hand counterpart (A); the 2D MD energies can be related by $E^{A'}_{\eta\eta'} = E^{A}_{\eta_-\eta'_-}$ (e.g., $E^{ldldl}_{T_-O_+} = E^{dldld}_{T_+O_-}$). The $E_{\eta\eta'}$ values of pentads (B′), nos. 5, 9, 11, 13, 14, and 15 in Table 1 are, respectively, obtained from those of pentads (B), nos. 3, 2, 6, 4, 12, and 8 in the same column by the relation $E^{B'}_{\eta\eta'} = E^{B}_{\eta'\eta}$ (e.g., $E^{dldld}_{O_-T_+} = E^{dldld}_{T_+O_-}$). Accordingly, the $E_{\eta\eta'}$ values of the above 10 pentads yield those of all of the pentads. The E_η value and dihedral angle (ϕ_η) of the η state of the mirror image (C′) of a tetrad (C) can be derived from $E^{C'}_\eta = E^{C}_{\eta_-}$ and $\phi^{C'}_\eta = -\phi^{C}_\eta$ (e.g., $E^{ldld}_T = E^{dldl}_{T_+}$ and $\phi^{ldld}_{T_-} = -\phi^{dldl}_{T_+}$). The E^{ddld}_η and E^{dddl}_η (ϕ^{ddld}_η and ϕ^{dddl}_η) values were obtained from $E^{ddld}_\eta = E^{dldd}_{\eta_-}$ and $E^{dddl}_\eta = E^{dlll}_\eta$ ($\phi^{ddld}_\eta = -\phi^{dldd}_{\eta_-}$ and $\phi^{dddl}_\eta = \phi^{dlll}_\eta$), respectively. The E_η and ϕ_η values of 16 tetrads can be derived from those of 6 tetrads (*dldl*, *dldd*, *dlld*, *dlll*, *ddll*, and *dddd*) shown in Supporting Information.

2.3. Computer Generation of the Atactic PMPrS Chain. Virtual chains including a variety of stereosequences were

TABLE 1: Pentads of PMPrS[a]

		d and *l*	
no.	*m* and *r*	A	A′
1	*rrrr*	*dldld*	*ldldl*
2	*rrrm*	*dldll*	*ldldd*
3	*rrmr*	*dlddl*	*ldlld*
4	*rrmm*	*dlddd*	*ldlll*
5	*rmrr*	*dlldl*	*lddld*
6	*rmrm*	*dlldd*	*lddll*
7	*rmmr*	*dllld*	*ldddl*
8	*rmmm*	*dllll*	*ldddd*
9	*mrrr*	*ddldl*	*lldld*
10	*mrrm*	*ddldd*	*lldll*
11	*mrmr*	*ddlld*	*llddl*
12	*mrmm*	*ddlll*	*llddd*
13	*mmrr*	*dddld*	*llldl*
14	*mmrm*	*dddll*	*llldd*
15	*mmmr*	*ddddl*	*lllld*
16	*mmmm*	*ddddd*	*lllll*

[a] For definitions of the *m* and *r* linkages and the *d* and *l* configurations, see Figure 2.

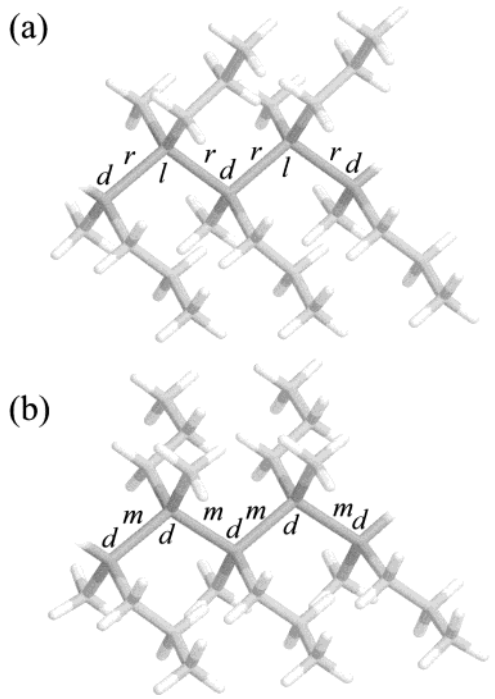

Figure 2. Stereoregular pentads of PMPrS: (a) syndiotactic (*dldld* or *rrrr*) and (b) isotactic (*ddddd* or *mmmm*) pentads. The stereosequences are defined according to the concept of pseudoasymmetry.[10,11,16,17] The silicon backbone is put on paper as shown. When the *n*-propyl group on the leftmost Si atom appears on this side of the paper, the Si site adopts the *d* form. Otherwise, the Si site is in the *l* form. For other Si sites, the *d* and *l* configurations are defined similarly. Here, *m* and *r* represent *meso* ($d \rightarrow d$ or $l \rightarrow l$) and *racemo* ($d \rightarrow l$ or $l \rightarrow d$) linkages, respectively.

generated by a computer, and their $\langle r^2\rangle_0/nl^2$ values were calculated according to the following procedures. (1) A number is sampled out of a set in which numbers are distributed uniformly between zero and unity. If the number is smaller than or equal to 0.5, then the leftmost Si site of the chain is set in the *d* form. Otherwise, the *l* form is assigned. (2) Similarly, a random number is generated. When the value is not larger than a given value of the *meso*-diad probability, P_m, then a monomeric unit is added to the chain terminal in the *meso* manner ($d \rightarrow d$ or $l \rightarrow l$). Otherwise, the monomer is added in the *racemo* manner ($d \rightarrow l$ or $l \rightarrow d$). (3) Geometrical parameters are chosen for the newly formed tetrad, and the statistical weight matrix is filled with $\sigma_{\eta\eta'}$ values corresponding to the terminal pentad. Procedures 2 and 3 are repeated up to a given degree of polymerization. (4) From a series of statistical weight matrices thus arranged, the characteristic ratio $\langle r^2\rangle_0/nl^2$ is calculated. The above process is performed for all chains in the system. (The number of chains is n_c.) The $\langle r^2\rangle_0/nl^2$ values of the n_c chains are averaged to be compared with the experimental value.

2.4. Molecular Dynamics Simulation. Rotational isomerizations in main and side chains of PSs are strongly interdependent. However, the equivalency between time and ensemble averages in statistical mechanics facilitates the evaluation of conformational energies. If an MD simulation for a PS with long alkyl side chains is performed with the dihedral angles of the main chain being fixed at given values, then the total energy averaged over a long time may represent the conformational energy weighted by the probabilities of side-chain conformations allowed there. Therefore, the positions and energies of the potential minima were determined from MD simulations for oligomeric model compounds and used in the RIS calculations.

Molecular dynamics simulations were carried out with the Cerius[2] package (Molecular Simulation, Inc.) installed on a Silicon Graphics Indigo2 workstation at AIST, Tsukuba. The polymer-consistent force fields optimized for PSs[19] and alkanes[20] were employed. Before MD computations were begun, the total energy was minimized with respect to geometrical parameters. The charge equilibration method[21] and the Ewald method[22] with a cutoff of 9 Å were used to calculate charge distributions and long-range electrostatic interactions, respectively. The NVT ensemble was assumed, and the time interval was set to 10 fs. The temperature was initially set at 600 K for 1 ps and decreased to 298.15 K. After 30 ps, the total energies were recorded at 10-fs intervals for 50 ps to outline energy maps and for 10 ns to search for the potential minima and evaluate conformational energies for the RIS calculations. In the latter case, the data collected for the last 5 ns were averaged to yield the energy parameters.

The spatial configuration of an unperturbed polymer has been considered to depend only on short-range intramolecular interactions.[10] Therefore, we carried out MD simulations for a single model compound in vacuo. In the cases of PDBS and PDHS, their decameric and undecameric model compounds, $Me[SiR_2]_{10}Me$ and $Me[SiR_2]_{11}Me$ (R: *n*-butyl or *n*-hexyl group), were adopted (Figure 3). The decamers were used to search for the potential minima around the central Si−Si bond to a precision of 0.1° and evaluate the first-order interaction energies, E_η, at the potential minima. For intervals of 30° for dihedral angles ϕ_{i-1} and ϕ_i of the central bonds of the undecamers, the MD simulation was performed, and the time-averaged energy was plotted as a function of ϕ_{i-1} and ϕ_i. The local minima were searched for on the energy map, and additional MD simulations were carried out in that neighborhood at intervals of 10° with ϕ_{i-1} and ϕ_i given a tolerance of ±5°. The time-averaged energy was considered to be the 2D energy, $E_{\eta\eta'}$. For PMPrS, the same procedure as that described above was adopted; however, the ϕ_η and E_η values were determined from 6 decamers $Me[SiMe_2]_3[SiMePr]_4[SiMe_2]_3Me$, and the $E_{\eta\eta'}$ values were determined from 10 undecamers $Me[SiMe_2]_3[SiMePr]_5[SiMe_2]_3Me$, where Pr represents an *n*-propyl group (Figure 4). Three $SiMe_2$ units are attached to both ends of the individual tetrads and pentads to prevent the *n*-propyl substituents from fanning out.

3. Results

3.1. PDBS and PDHS. Energy contour maps obtained from the undecamers of PDBS and PDHS are shown in Figure 5.

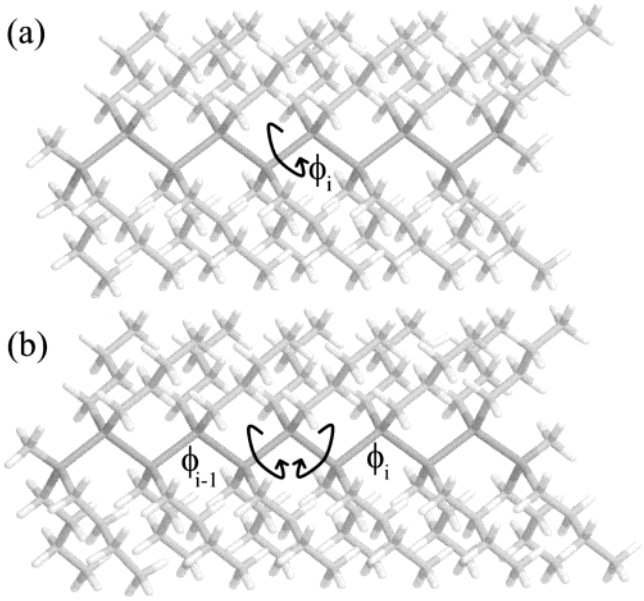

Figure 3. Model compounds of PDBS used in MD simulations: (a) decamer and (b) undecamer in the all-anti conformation. The dihedral angles, ϕ_i and ϕ_{i-1}, are defined for the central bond(s).

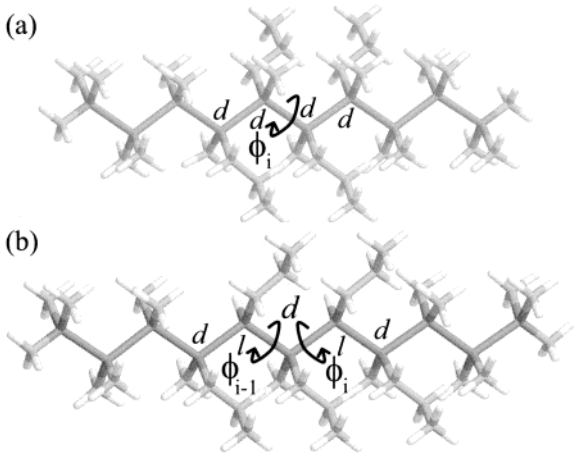

Figure 4. Examples of model compounds of PMPrS used in MD simulations: (a) decamer with a *dddd* (*mmm*) tetrad and (b) undecamer with a *dldld* (*rrrr*) pentad in the all-anti conformation. The dihedral angles, ϕ_i and ϕ_{i-1}, are defined for the central bond(s).

The local minima can be found around ϕ_i (or ϕ_{i-1}) = ±150° ($D_\pm$), ±90° ($O_\pm$), and ±70° ($G_\pm$) on the line ϕ_{i-1} (or ϕ_i) = ±150°($D_\pm$). Potential wells of PDHS are more concentrated than those of PDBS; an increase in the side-chain length by two methylene units significantly reduces the allowable ranges of ϕ_{i-1} and ϕ_i. Dihedral angles and conformational energies, evaluated from more detailed computations, are listed in Table 2. Only conformations related to $D_\pm$ states have energies smaller than 10 kcal mol^{-1}; the other conformations may be negligible. Most of the two consecutive Si−Si bonds are suggested to adopt one of four states: D_+D_+, D_-D_-, D_+D_-, or D_-D_+.[23]

Characteristic ratios of PDBS at 19.1 °C and PDHS at 25.0 °C (the Θ conditions)[2] were calculated from the ϕ_η, E_η, and $E_{\eta\eta'}$ values. There, bond lengths l_{Si-Si} and bond angles ∠SiSiSi were set to 2.35 Å and 115.4°, respectively.[1,24] In Figure 6, calculated $\langle r^2\rangle_0/nl^2$ values are plotted against the reciprocal of the degree (x) of polymerization. The data are located on the individual lines, of which intercepts at $x^{-1} = 0$ yield $\langle r^2\rangle_0/nl^2$ values at $x = \infty$: 42.0 for PDBS and 54.0 for PDHS.

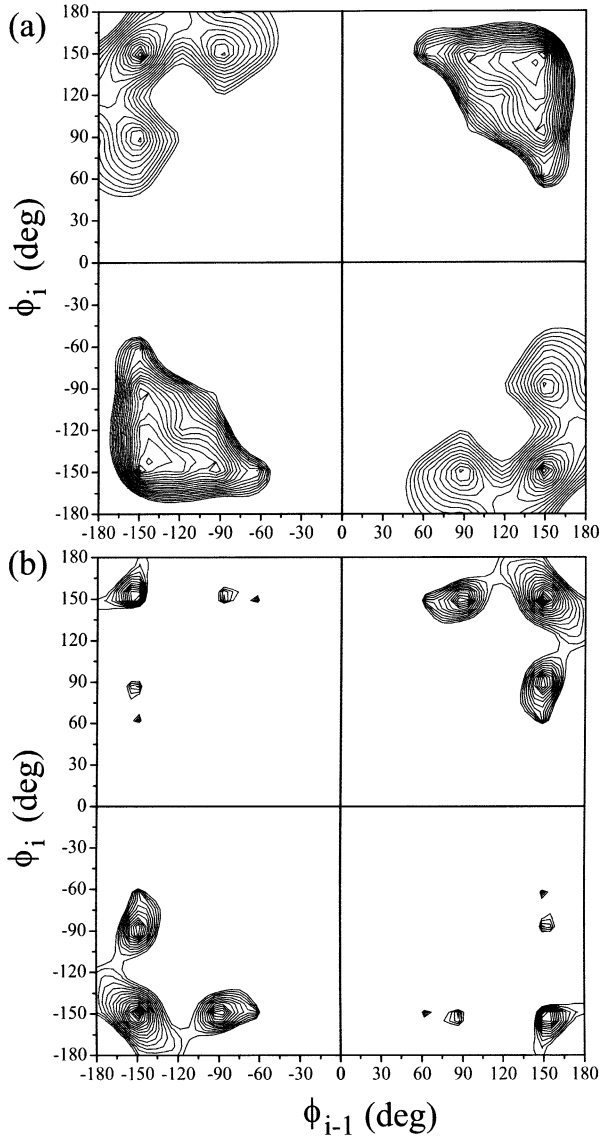

Figure 5. Energy contour maps of the undecamers of (a) PDBS and (b) PDHS. The contour lines are drawn at intervals of 0.5 kcal mol^{-1}.

Experimental $\langle r^2\rangle_0/nl^2$ values for PDBS and PDHS are 42.3 ± 4.2 and 42.5 ± 3.9, respectively. Here, the error margins were estimated from the standard deviations and systematic errors of the light-scattering experiments.[25] The RIS calculations exactly reproduced the experiment for PDBS but only moderately reproduced the experiment for PDHS.

Listed in Table 3 are the first derivatives $(\partial(\langle r^2\rangle_0/nl^2)/\partial X)$ of the characteristic ratio of PDBS with respect to the geometrical and energy parameters (X). A large differential coefficient is found for $E_{D_\pm D_\mp}$, of which variation significantly affects the $\langle r^2\rangle_0/nl^2$ calculation. This is because most Si−Si bond pairs adopt either $D_\pm D_\pm$ or $D_\pm D_\mp$ conformations. Accordingly, at least, this energy parameter may be exactly determined so as to reproduce the experimental $\langle r^2\rangle_0/nl^2$ value. Figure 7 shows the characteristic ratio of PDBS as a function of $E_{D_\pm D_\mp}$. The relation is also applicable to PDHS because its geometrical and energy parameters evaluated from the MD simulations are very close to those of PDBS, as shown in Table 2.[27] In Figure 7, the calculated curve intersects the horizontal lines representing the observations at $E_{D_\pm D_\mp} = 0.12$ kcal mol^{-1}. If the error margins of $\langle r^2\rangle_0/nl^2$ are considered, then the optimal value is given as $E_{D_\pm D_\mp} = 0.12 \pm 0.07$ kcal mol^{-1} for both PDBS and PDHS. It is preferable that

TABLE 2: Dihedral Angles and Energy Parameters of PDBS and PDHS as Evaluated from MD Simulations and Corresponding Calculated Characteristic Ratios

dihedral angle, deg	PDBS	PDHS
$\phi_{D_\pm}$	±151.5	±151.7
$\phi_{O_\pm}$	±92.3	±92.3
$\phi_{G_\pm}$	±71.5	±72.3
MD energy,[a] kcal mol^{-1}	**PDBS**	**PDHS**
$E_{D_\pm}$	0.00	0.00
$E_{O_\pm}$	1.85	2.00
$E_{G_\pm}$	2.18	2.52
$E_{D_\pm D_\pm}$	0.00	0.00
$E_{D_\pm D_\mp}$	0.11	0.23
$E_{D_\pm O_\pm}$	2.12	2.39
$E_{D_\pm O_\mp}$	2.59	2.95
$E_{D_\pm G_\pm}$	2.91	2.78
$E_{D_\pm G_\mp}$	2.59	3.58
$E_{O_\pm O_\pm}$	>10	>10
$E_{O_\pm O_\mp}$	>10	>10
$E_{O_\pm G_\pm}$	>10	>10
$E_{O_\pm G_\mp}$	>10	>10
$E_{G_\pm G_\pm}$	>10	>10
$E_{G_\pm G_\mp}$	>10	>10
$\langle r^2\rangle_0/nl^{2b}$	42.0[c]	54.0[d]

[a] Relative to $E_{D_\pm}$ or $E_{D_\pm D_\pm}$. [b] Calculated from the dihedral angles, MD energies, l_{Si-Si} of 2.35 Å, and ∠SiSiSi of 115.4°. [c] For PDBS of $x = \infty$ at 19.1 °C. See Figure 6. [d] For PDHS of $x = \infty$ at 25.0 °C.

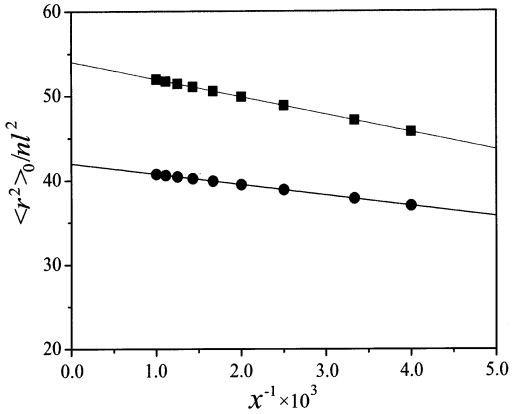

Figure 6. Characteristic ratios of PDBS (●) and PDHS (■) as a function of the reciprocal of degree (x) of polymerization. The intercept at $x^{-1} = 0$ corresponds to the $\langle r^2\rangle_0/nl^2$ at $x = \infty$: PDBS, 42.0; PDHS, 54.0.

the $E_{D_\pm D_\mp}$ value should be represented as ca. 0.1 kcal mol^{-1}. From the above results, as a crude approximation, the statistical weight matrices for PDBS and PDHS may be reduced to

$$U_2 = \begin{array}{c} \\ \mathrm{D}_+ \\ \mathrm{D}_- \end{array} \begin{array}{c} \begin{array}{cc} \mathrm{D}_+ & \mathrm{D}_- \end{array} \\ \begin{pmatrix} 1 & 1 \\ 0 & 0 \end{pmatrix} \end{array} \tag{3}$$

and

$$U_i = \begin{array}{c} \\ \mathrm{D}_+ \\ \mathrm{D}_- \end{array} \begin{array}{c} \begin{array}{cc} \mathrm{D}_+ & \mathrm{D}_- \end{array} \\ \begin{pmatrix} 1 & \sigma_{D_+D_-} \\ \sigma_{D_-D_+} & 1 \end{pmatrix} \end{array} \tag{4}$$

where $\sigma_{D_\pm D_\mp} = \exp(-E_{D_\pm D_\mp}/RT)$.

3.2. PMPrS. Locations of the potential minima of PMPrS depend on the microstructure. In Figure 8, as an example, the energy contour map of the *ddddd* pentad is shown. The six-state scheme is seen to be applicable to this pentad. This approximation is, in general, valid for the other pentads.[30]

TABLE 3: First Derivatives[a] of Characteristic Ratios of PDBS with Respect to Geometrical and Energy Parameters (X)

X	$\partial(\langle r^2\rangle_0/nl^2)/\partial X$
∠SiSiSi	1.5
$\phi_{D_\pm}$	2.7
$\phi_{O_\pm}$	0.061
$\phi_{G_\pm}$	0.023
$E_{O_\pm}$	−3.2
$E_{G_\pm}$	−3.6
$E_{D_\pm D_\mp}$	53
$E_{D_\pm O_\pm}$	2.0
$E_{D_\pm O_\mp}$	4.3
$E_{D_\pm G_\pm}$	1.7
$E_{D_\pm G_\mp}$	5.7

[a] In deg^{-1} for the geometrical parameters and in kcal^{-1} mol for the energy parameters. The other parameters were set as obtained from the MD simulations. A variation in l_{Si-Si} has no effect on the calculated $\langle r^2\rangle_0/nl^2$ value. Energy parameters other than those shown above are too large to yield essentially null $\partial(\langle r^2\rangle_0/nl^2)/\partial X$ values.

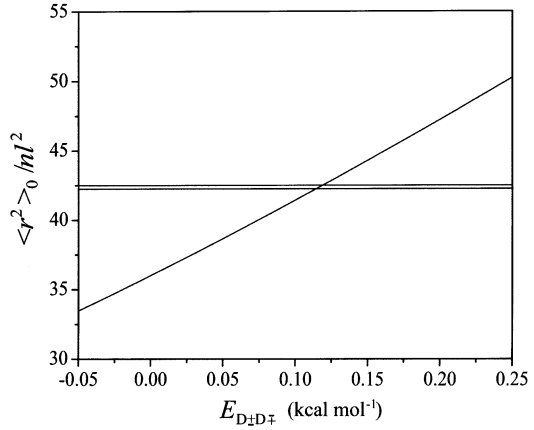

Figure 7. Variation in the characteristic ratio of PDBS with $E_{D_\pm D_\mp}$. The horizontal lines represent the observations: 42.3 for PDBS and 42.5 for PDHS.

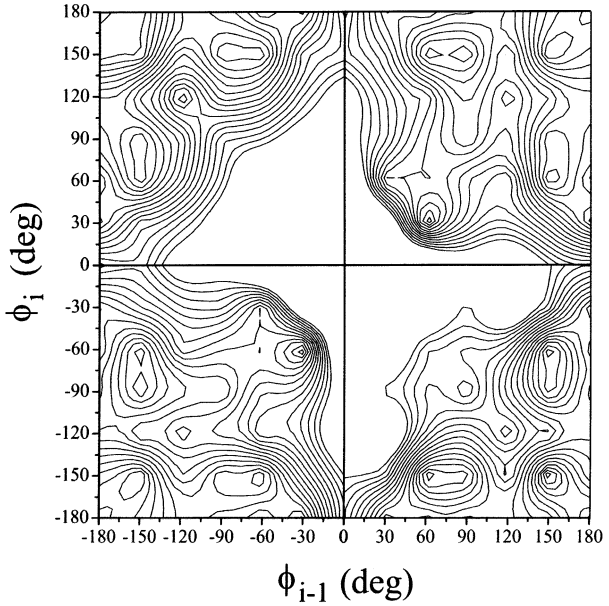

Figure 8. Energy contour map for the *ddddd* (*mmmm*) pentad of PMPrS. The contour lines are drawn at intervals of 0.5 kcal mol^{-1}.

In Figure 9, characteristic ratios of PMPrS chains of different x and n_c values, calculated as above, are plotted against x^{-1}. In the RIS calculations, the ϕ_η, E_η, and $E_{\eta\eta'}$ values obtained from

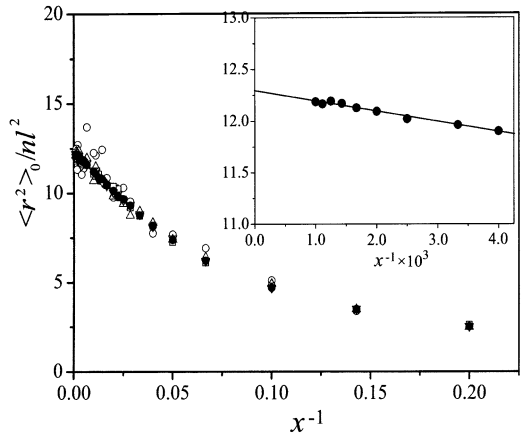

Figure 9. Characteristic ratios of atactic PMPrS chains with different numbers of chains sampled n_c as a function of x^{-1}: $n_c = 1$ (○), 4 (△), 16 (□), 64 (▽), and 256 (●). The *meso*-diad probability, P_m, was set equal to 0.5. In the upper right corner, the plot for $n_c = 256$ is extended. The intercept at $x^{-1} = 0$ gives a $\langle r^2\rangle_0/nl^2$ value of 12.3.

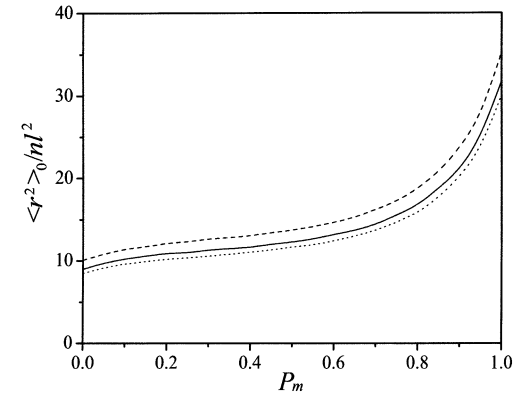

Figure 10. Characteristic ratio of PMPrS for $x = \infty$ and $n_c = 256$ as a function of P_m: (···) ∠SiSiSi = 114.0°, (—) ∠SiSiSi = 115.4°, and (- - -) ∠SiSiSi = 118.0°.

MD simulations (Supporting Information), $l_{Si-Si} = 2.35$ Å, and ∠SiSiSi = 115.4° were used. By ^{29}Si NMR for PMPrS,[31,32] a number of signals coming from different configurations were observed. The stereosequences are considered to be formed according to Bernoulli trials; however, the *meso*-diad probability, P_m, has not been experimentally determined. Here, the PMPrS chain was assumed to be completely atactic; that is, P_m was set to equal to 0.50. When n_c is small, the data are scattered because the samplings are not large enough to satisfy $P_m = 0.50$. When n_c is 256, the calculated $\langle r^2\rangle_0/nl^2$ values, represented by filled circles, seem to form a smooth curve and converge to 12.3 at $x^{-1} = 0$ ($x = \infty$). This value is smaller than the observations of 19.9 ± 2.2.[2,25] An X-ray crystallographic analysis of PMPrS[33] has given $l_{Si-Si} = 2.36$ Å and ∠SiSiSi = 116 ± 2°. For ∠SiSiSi = 114.0, 115.4, and 118.0°, therefore, the P_m dependence of $\langle r^2\rangle_0/nl^2$ was investigated using geometrical and energy parameters as obtained from the MD simulations. In Figure 10, the characteristic ratio is expressed as a function of P_m. The $\langle r^2\rangle_0/nl^2$ value gradually increases with P_m: $P_m = 0.0$ (syndiotactic), 8.5−10.1; $P_m = 1.0$ (isotactic), 30.1−35.3. Thus, the *meso* linkage renders the asymmetric PS chain extended. If we accept the $\langle r^2\rangle_0/nl^2$ versus P_m curves as they are, the experimental values of 19.9 ± 2.2 correspond to $P_m = 0.76-0.92$; the *meso* linkage, which is free from the steric hindrance between longer *n*-propyl side chains, may be preferred. This problem will be discussed in the final section.

4. Discussion

4.1. Order−Disorder Transition. It is known that PSs exhibit an order−disorder transition before degradation.[1,34] For example, PDMS, PDBS, poly(di-*n*-pentyl)silane (PDPS), and PDHS change the crystal structure (phase I) to a conformational disordering ("condis") state (phase II) at 157, 87, 65, and 50 °C, respectively.[6,34−36] The latter state, being analogous to the rotator phase of *n*-alkanes,[37] is considered to be a liquid crystalline state in a broad sense[38] in which the PS chain is considerably rigid and hence far from a random coil. ^{13}C NMR spectra observed from PDHS are markedly changed at the disordering transition, and the chemical shifts of phase II correspond to those of the solutions.[36] From ^{29}Si and ^{13}C NMR relaxation times, both the main and side chains of PDBS, PDPS, and PDHS in the condis phase were shown to move on the same time scale irrespective of side-chain length.[34] Our variable-temperature IR measurements of PDBS and PDHS have indicated that well-defined Si−C rocking bands assigned to specific conformations, observed at low temperatures, become considerably broadened after the disordering transition; the main and side chains begin cooperative motions around the transitional temperature.[39]

At the order−disorder transition, an endothermic peak is observed by DSC. Wunderlich's group[34] has evaluated the disordering entropies (ΔS_d) of PDPS and PDHS of 100% crystallinity as 3.04 and 18.0 cal K^{-1} mol^{-1}, respectively. The net contribution of the backbone to ΔS_d was estimated to be ca. 2 cal K^{-1} mol^{-1}. The large ΔS_d value of PDHS undoubtedly comes from the melting of crystalline side chains.

According to the RIS scheme, the configurational entropy of the backbone per mole of monomers can be calculated from[40−42]

$$S_{conf} = R\left(\ln z + T\frac{\mathrm{d}\ln z}{\mathrm{d}T}\right) \tag{5}$$

where z is the configurational partition function per monomeric unit, given by

$$z = Z^{1/x} \tag{6}$$

with Z being the partition function of the whole chain. The Z function is calculated from

$$Z = \mathbf{J}^*\left(\prod_{i=2}^{x-1} U_i\right)\mathbf{J} \tag{7}$$

where $\mathbf{J}^* = [100000]$ and $\mathbf{J}$ is the 6×1 column matrix whose elements are unity. The statistical weight matrices U_i are scaled so that the weight of the lowest-energy conformation is unity. The S_{conf} values of PDBS and PDHS, calculated from the MD energies, are 1.5 cal K^{-1} mol^{-1}. Then, the $E_{D_\pm D_\mp}$ values were set to 0.1 kcal mol^{-1}. The ΔS_d term includes the configuration entropy of the side chains and the entropy due to volume change as well as S_{conf}. The small S_{conf} value of 1.5 cal K^{-1} mol^{-1} represents the inherent rigidity of PDBS and PDHS chains, which are allowed to adopt only D± conformations even in the Θ state. This is the reason for the liquid crystallinity of phase II; steric repulsions between the long side chains compel the backbone to be extended and rotate along the molecular axis with ϕ_i being kept at ca. ±150°. In the U_i matrices of eq 7, the weight of the lowest-energy state is defined as unity. Thus, the most stable state corresponding to $Z = 1$ (i.e., $S_{conf} = 0$) is either $D_+D_+...D_+$ or $D_-D_-...D_-$, which forms the 7/3 helical structure. It should be noted that the S_{conf} value calculated from eq 5 represents the conformational change from the 7/3 helical

structure to the Θ state; the structural change between the all-anti and 7/3 helical structure, being characteristic of PDHS, is not included. In phase II, the PS chains may deviate somewhat from the Θ state. Because of the small energy difference of ca. 0.1 kcal mol^{-1} between $D_{\pm}D_{\pm}$ and $D_{\pm}D_{\mp}$, the $D_{\pm}D_{\mp}$ conformations must be left in the crystal, play the role of defect, and reduce the crystallinity. In solid-state ^{32}Si NMR spectra of PDBS and PDHS at room temperature, resonances from phases I and II are intermingled.[6, 36]

In the case of PMPrS, a variety of conformational pairs including $O_{\pm}$ and $G_{\pm}$ states are permitted to exist in the Θ state.[43] Thus, the PMPrS chain in the molten state and in solution may be closer to a random coil rather than a liquid crystal. The melting point of PMPrS, depending on molecular weight, ranges from 44 to 55 °C.[44]

4.2. UV Absorption and Backbone Conformation. As stated in the Introduction, the λ_{max} value depends on the backbone conformation. A number of theoretical studies have attempted to relate λ_{max} to ϕ_i.[1] For example, a tight-binding model[45] leads to the band gap E_g between the highest occupied and lowest unoccupied states in the form of $E_g = \alpha(\beta - \gamma \cos \phi_i)$, where α, β, and γ are independent of ϕ_i. If $\lambda_{max} \propto E_g^{-1}$ is assumed, then the ϕ_i dependence of λ_{max} may be outlined by trigonometric functions. From the geometrical and energy parameters of PDBS, PDHS, and PMPrS, we attempted to derive a relationship between λ_{max} and ϕ_i on PSs with alkyl side chains. In solutions and melts (or disordered phases), the PS chains undergo rapid conformational changes. Therefore, the observed UV absorption, coming from a large number of conformations, must be correlated with the average dihedral angle.

The average dihedral angle $\langle|\phi|\rangle$ can be calculated from

$$\langle|\phi|\rangle = \frac{1}{n_c(x-2)} \sum_{k=1}^{n_c} \sum_{i=2}^{x-1} \sum_{\eta} |\phi_{i;\eta}^k| p_{i;\eta}^k \qquad (8)$$

where $\phi_{i;\eta}^k$ and $p_{i;\eta}^k$ are the dihedral angle and probability ($\sum_\eta p_{i;\eta}^k = 1$) of the η state of the ith Si−Si bond of the kth chain, respectively. The conformational probability can be calculated from the statistical weight matrices according to the RIS scheme. Because Si−Si bonds of PMPrS have different stereosequences, the summation of eq 8 must be performed over $(x - 2)$ bonds of n_c chains. For PDBS and PDHS, on the other hand, eq 8 can be simplified to

$$\langle|\phi|\rangle = \sum_{\eta} |\phi_\eta| p_\eta \qquad (9)$$

where p_η is the average fraction (bond conformation) of the η state. The $\langle|\phi|\rangle$ values for the Θ state were obtained as follows: PDBS, 150.6°; PDHS, 151.2°; PMPrS, 139.6° for ∠SiSiSi = 115.4° (for example), $P_m = 0.5$, $x = 1000$, and $n_c = 256$ and 146.0° for ∠SiSiSi = 118.0°, $P_m = 0.83$, $x = 1000$, and $n_c = 256$.[43] Because crystallized PDBS and PDHS chains adopt the 7/3 helical and all-anti structures, respectively, the corresponding $\langle|\phi|\rangle$ values are 151.5 and 180.0°. Trans conformations of PMPrS are not the most stable in all of the pentads but are of comparable low energy (Supporting Information). X-ray diffraction studies on PMPrS[33,44,46] have indicated that all of the Si−Si bonds take trans conformations (A, T, and D). If the dihedral angles in the Θ state are kept even in the solid, then the $\langle|\phi|\rangle$ value of solid PMPrS chains can be calculated to be 165.5°. In Figure 11, the λ_{max} values obtained from Figure 1 are plotted against $\langle|\phi|\rangle$. On the vertical line of $\langle|\phi|\rangle = 0$, however, the λ_{max} value of 374 nm is plotted instead of λ_{max} = 363 nm.[3,47] The data, collected from three PSs, appear to form a master curve.

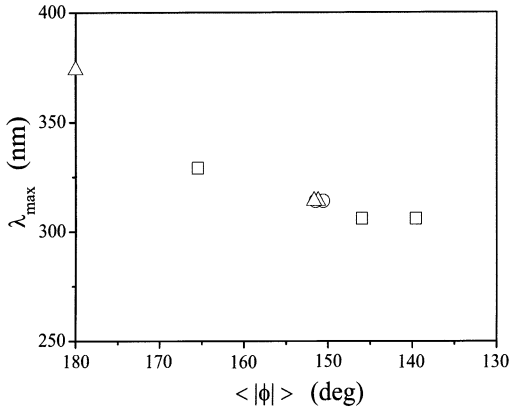

Figure 11. Correlation between UV absorption maximum (λ_{max}) and average dihedral angle ($\langle|\phi|\rangle$): (○) PDBS, (△) PDHS, and (□) PMPrS.

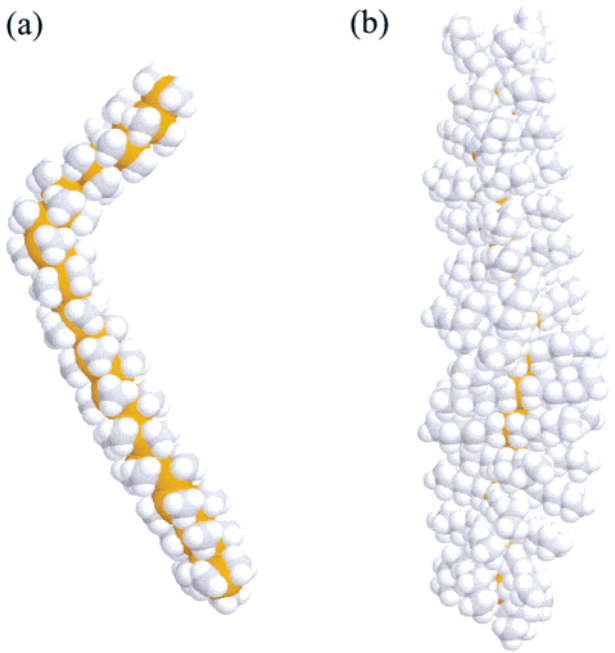

Figure 12. Schematic illustration of (a) PDMS and (b) PDHS chains in the disordered phase and in solution.

On cooling, PDBS and PDHS in solution suddenly change their λ_{max} value from ca. 320 to 355 nm at −36 and −31 °C, respectively.[6,7] A similar phenomenon was observed from an end-grafted PDHS film.[48] The $\langle|\phi|\rangle$ value corresponding to λ_{max} = 355 nm can be estimated from Figure 11 as ca. 175°. For PDBS and PDHS, a large change in heat capacity, corresponding to the glass transition, was observed around these temperatures;[6,34] the frozen side chains may allow the backbone to untwist from the deviant to anti region.

4.3. Solubility of PSs. The S_{conf} value of PDMS at the disordering transition (157 °C) was calculated from eq 5 as 2.7−2.9 cal K^{-1} mol^{-1} using energy parameters offered by Michl's group,[49] being within the ΔS_d range (1.7−2.9 cal K^{-1} mol^{-1}) estimated by Wunderlich's group.[34] This is reasonable because the methyl substituent does not yield configurational entropy (Figure 12a). It has been suggested that an isolated PDMS chain can take $G_{\pm}$ conformations;[13−15] therefore, PDMS is more flexible than PDHS (S_{conf} = 1.5 cal K^{-1} mol^{-1}). Nevertheless, PDMS is insoluble in almost all solvents, whereas PDHS is soluble in a number of solvents. The solubility of PDHS is obviously due to the configurational entropy of the long side

chain. From Figure 12b, it is seen that solvents can hardly recognize the existence of the Si backbone behind hexyl side chains. For example, a good solvent, *n*-hexane, feels as if the PDHS chain were a group of *n*-hexane molecules of low translational mobility, and the mixing is athermal as if hexane is dissolved in hexane. Thus, the driving force of solubility is not enthalpy but entropy. *n*-Hexane is a good solvent for PDHS but a Θ solvent for PDBS (at 19.1 °C). Whether *n*-hexane is a good or Θ solvent is due to the configurational entropy difference caused by two methylene units of the side chain.

5. Concluding Remarks

A methodology for conformational analyses of polymers with long side chains has been presented. As shown above, the RIS calculations with MD simulations for PDBS and PDHS have successfully correlated their configurations and conformations with higher-order structures and thermal, optical, and solution properties; therefore, the computational method proposed here has been demonstrated to be acceptable.

However, if the stereosequence of PMPrS results from the completely random Bernoulli trials of $P_m = 0.5$, the agreement in $\langle r^2\rangle_0/nl^2$ between theory and experiment is not satisfactory. Because a large number of geometrical and energy parameters are used for PMPrS, the definite cause cannot be easily found. However, we should remember some simplifications adopted here. For example, the six-state approximation may not be applied to all of the tetrads and pentads. The Θ state occurs at a specific composition of the mixed solvents (*n*-hexane (62.6%) and 2-propanol (37.4%) at 25 °C). The force fields employed here[19] are based on ab initio molecular orbital calculations for silanes in vacuo. Thus, solvent effects are not included in the present computations. Short side chains of methyl and propyl groups allow the solvents to interact directly with the main chain. Therefore, incorporating the solvents as well as the oligomeric models into the MD simulations will enable a more precise reproduction of the experiment.

Because the energy data were collected in the MD simulations with ϕ_{i-1} and ϕ_i set to given values, the RIS treatment represents only statically equilibrated states. In dynamic processes (e.g., transitions between conformations), the main and side chains will collaborate to find a path of lower energy than that presented here.

Acknowledgment. We thank the following people for valuable advice and hearty encouragement: Dr. Tanabe, Dr. Kinugasa, Dr. Tanigaki, Dr. Kyotani, Dr. Saito, Dr. Mikami, and Dr. Tsuzuki of AIST and Professor Kitamura, Professor Karatsu, and Professor Akutsu of Chiba University. This work was supported in part by a Grant-in-Aid for Scientific Research (C) (no. 14550842) of the Japan Society for the Promotion of Science.

Supporting Information Available: ϕ_η and E_η values of 6 tetrads and $E_{\eta\eta'}$ values of 10 pentads of PMPrS. This material is available free of charge via the Internet at http://pubs.acs.org.

References and Notes

(1) See, for example, Miller, R. D.; Michl, J. *Chem. Rev.* **1989**, *89*, 1359 and references therein.

(2) Kato, H.; Sasanuma, Y.; Kaito, A.; Tanigaki, N.; Tanabe, Y.; Kinugasa, S. *Macromolecules* **2001**, *34*, 262.

(3) Rabolt, J. F.; Hofer, D.; Miller, R. D.; Fickes, G. N. *Macromolecules* **1986**, *19*, 611.

(4) Lovinger, A. J.; Schilling, F. C.; Bovey, F. A.; Zeigler, J. M. *Macromolecules* **1986**, *19*, 2657.

(5) Kuzmany, H.; Rabolt, J. F.; Farmer. B. L.; Miller, R. D. *J. Chem. Phys.* **1986**, *85*, 7413.

(6) Schilling, F. C.; Lovinger, A. J.; Zeigler, J. M.; Davis, D. D.; Bovey, F. A. *Macromolecules* **1989**, *22*, 3055.

(7) Harrah, L. A.; Zeigler, J. M. *J. Polym. Sci., Polym. Lett. Ed.* **1985**, *23*, 209.

(8) Michl, J.; West, R. *Acc. Chem. Res.* **2000**, *33*, 821.

(9) *Pure Appl. Chem.* **1976**, *45*, 11. *Pure Appl. Chem.* **1981**, *53*, 733.

(10) Flory, P. J. *Statistical Mechanics of Chain Molecules*; Interscience: New York, 1969.

(11) Mattice, W. L.; Suter, U. W. *Conformational Theory of Large Molecules: The Rotational Isomeric State Model in Macromolecular Systems*; Wiley & Sons: New York, 1994.

(12) Abe, A.; Jernigan, R. L.; Flory, P. J. *J. Am. Chem. Soc.* **1966**, *88*, 631.

(13) Neumann, F.; Teramae, H.; Downing, J. W.; Michl, J. *J. Am. Chem. Soc.* **1998**, *120*, 573.

(14) Albinsson, B.; Antic, D.; Neumann, F.; Michl, J. *J. Phys. Chem. A* **1999**, *103*, 2184.

(15) Ottosson, C.; Michl. J. *J. Phys. Chem. A* **2000**, *104*, 3367.

(16) Flory, P. J.; Mark, J. E.; Abe, A. *J. Am. Chem. Soc.* **1966**, *88*, 639.

(17) Flory, P. J. *J. Am. Chem. Soc.* **1967**, *89*, 1798.

(18) Metanomski, W. V. *Compendium of Macromolecular Nomenclature*; Blackwell Science: Cambridge, MA, 1991.

(19) Sun, H. *Macromolecules* **1995**, *28*, 701.

(20) Hwang, M. J.; Stockfisch, T. P.; Hagler, A. T. *J. Am. Chem. Soc.* **1994**, *116*, 2515.

(21) Rappé, A. K.; Goddard, W. A., III. *J. Phys. Chem.* **1991**, *95*, 3358.

(22) Frenkel, D.; Smit, B *Understanding Molecular Simulation: From Algorithms to Applications*; Academic Press: New York, 2002; Chapter 12.

(23) Bond conformations of unperturbed PDBS at 19.1 °C and PDHS at 25.0 °C were evaluated as follows: $p_{D_\pm} = 0.493$, $p_{O_\pm} = 0.005$, and $p_{G\pm} = 0.002$; $p_{D_\pm D_\pm} = 0.267$ and $p_{D_\pm D_\mp} = 0.219$.

(24) Welsh, W. J.; DeBolt, L.; Mark, J. E. *Macromolecules* **1986**, *19*, 2978.

(25) The error margins of $\langle r^2\rangle_0/nl^2$ were estimated from $\delta(\langle r^2\rangle_0/nl^2) = (\sigma_1^2 + \sigma_2^2)^{1/2}$, where σ_1 is the standard deviation of the experimental data and σ_2 is the systematic error in the light-scattering experiment.[26] The latter was supposed to be 9% of the observed value. (See note 24 of ref 2.) The degrees of polymerization of PDBS, PDHS, and PMPrS samples used in the light-scattering measurements were estimated to be $2.7 \times 10^3-1.6 \times 10^4$, $3.0 \times 10^3-1.4 \times 10^4$, and $2.0 \times 10^3-8.9 \times 10^3$, respectively.

(26) Taylor, J. R. *An Introduction to Error Analysis: The Study of Uncertainties in Physical Measurements*, 2nd ed.; University Science Books: Herndon, VA, 1997; Chapter 4.

(27) On the energy maps, the local minima of PDHS are more concentrated than those of PDBS. To correct the statistical weight for the angular distribution of energy, the preexponential factor has been introduced into the RIS scheme.[28] When the difference in energy between conformations is small, however, the deviation from the ordinary RIS treatment, which assumes the angular distribution to be a point, is negligible.[29] Because the energy difference between the $D_\pm D_\pm$ and $D_\mp D_\mp$ states is as small as 0.1 kcal mol^{-1}, the correction was not employed here.

(28) Suter, U. W.; Flory, P. J. *Macromolecules* **1975**, *8*, 765.

(29) Tasaki, K.; Sasanuma, Y.; Ando, I.; Abe, A. *Bull. Chem. Soc. Jpn.* **1984**, *57*, 2391.

(30) The MD simulations were carried out for all 36 conformers, although local minima were not always observed clearly. Such saddle points are so large in energy that they do not contribute anything to the calculated configuration-dependent properties.

(31) Schlling, F. C.; Bovey, F. A.; Zeigler, J. M. *Macromolecules* **1986**, *19*, 2309.

(32) Wolff, A. R.; Maxka, J.; West, R. *J. Polym. Sci., Polym. Chem. Ed.* **1988**, *26*, 713.

(33) Chunwachirasiri, W.; Kanaglekar, I.; Winokur, M. J.; Koe, J. C.; West, R. *Macromolecules* **2001**, *34*, 6719.

(34) Varma-Nair, M.; Cheng, J.; Jin, Y.; Wunderlich, B. *Macromolecules* **1991**, *24*, 5442.

(35) Lovinger, A. J.; Davis, D. D.; Schilling, F. C.; Padden, F. J., Jr.; Bovey, F. A.; Zeigler, J. M. *Macromolecules* **1991**, *24*, 132.

(36) Schlling, F. C.; Bovey, F. A.; Lovonger, A. J.; Zeigler, J. M *Macromolecules* **1986**, *19*, 2660.

(37) Ewen, B.; Strobl, G. R.; Richter, D. *Faraday Discuss. Chem. Soc.* **1980**, *69*, 19.

(38) Weber, P.; Guillon, D.; Skoulios, A.; Miller, R. D. *J. Phys. (Paris)* **1989**, *50*, 793.

(39) Kato, H. M.S. Thesis, Chiba University, Chiba, Japan, 2000.

(40) Brant, D. A.; Miller, W. G.; Flory, P. J. *J. Mol. Biol.* **1967**, *23*, 47.

(41) Tonelli, A. E. *J. Chem. Phys.* **1970**, *52*, 4749.

(42) Mark, J. E. *J. Chem. Phys.* **1977**, *67*, 3300.

(43) Bond conformations of unperturbed PMPrS were evaluated as follows: $p_{T+} = p_{T-} = 0.34$, $p_{O+} = p_{O-} = 0.10$, and $p_{G+} = p_{G-} = 0.06$ for $P_m = 0.5$ (and $\angle$SiSiSi = 115.4°); $p_{T+} = p_{T-} = 0.40$, $p_{O+} = p_{O-} = 0.07$, and $p_{G+} = p_{G-} = 0.03$ for $P_m = 0.83$ (and $\angle$SiSiSi = 118.0°). The former and latter parameters yield $\langle r^2\rangle_0/nl^2$ values of 12.3 and 19.9 at $x = \infty$, respectively.

(44) Jambe, B.; Jonas, A.; Devaux, J. *J. Polym. Sci., Part B: Polym. Phys.* **1997**, *35*, 1533.

(45) Mintmire, J. W. *Phys. Rev. B* **1989**, *39*, 13350.

(46) KariKari, E. K.; Greso, A. J.; Farmer, B. L.; Miller, R. D.; Rabolt, J. F. *Macromolecules* **1993**, *26*, 3937.

(47) Chunwachirasiri, W.; Kanaglekar, I.; Lee, G. H.; West, R.; Winokur, M. J. *Synth. Met.* **2001**, *119*, 31.

(48) Furukawa, K.; Ebata, K. *Macromolecules* **2002**, *35*, 327.

(49) Estimated from the E'' values in Table 5 of ref 15. The energy parameters evaluated from ab initio molecular orbital calculations at the HF/6-31G(d)//HF/3-21G(d) and MP2/6-31G(d)//HF/3-21G(d) levels gave S_{conf} values of 2.7 and 2.9 cal K^{-1} mol^{-1} at 157 °C, respectively.